National Aeronautics and Space Administration
Research Grant NAG-1-01032

Final Report for Research Titled

Design Study of a Synthetic Thinned Aperture Radiometer for Hurricane Impact Prediction

6 February 2003

Covering the period 1 April 2001 through 30 June 2002

Principal Investigator:

Christopher S. Ruf
Department of Atmospheric, Oceanic & Space Sciences
1521C Space Research Building
2455 Hayward Ave.
University of Michigan
Ann Arbor, MI 48109-2143
Voice: 734-764-6561
FAX: 734-764-5137
EMail: cruf@umich.edu

Title: Design Study of a Synthetic Tnhinned Aperture Radiometer for Hurricaner Impact Prediction
NASA Grant NAG-1-01032
Date: 6 February 2003
Prepared by: Christopher S. Ruf (PI)
Department of Atmospheric, Oceanic & Space Sciences
University of Michigan, Ann Arbor
734-764-6561 (V), 734-764-5137 (F), cruf@umich.edu (E)

Table of Contents

1. Summary of Final Report

This final report presents the results of work performed under NASA Grant NAG-1-01032 during the period 1 April 2001 through 30 June 2002. The principle accomplishments involve a conceptual design of an airborne Hurricane Imaging (microwave) Radiometer (HiRad) instrument for use in operational hurricane surveillance. The basis of the HiRad design is the Stepped Frequency Microwave Radiometer (SFMR) that has successfully measured surface wind speed and rain rate in hurricanes from the NOAA Hurricane Research Division's P-3 aircraft. Unlike the SFMR that views only at nadir, the HiRad provides wide-swath measurements between ± 45 degress in incidence angle with a spot-beam spatial resolution of approximately 1-3 km. The system operates at four equally spaced frequency channels that cover a range between 4 GHz and 6 GHz.

The final report consists of two parts. Part 1 is a reprint of a conference proceeding presented at the 2002 International Geoscience and Remote Sensing Symposium and authored by the principle members of the HiRad design team. Part 2 is a summary of the MMIC receiver design developed to support the HiRad sensor.

2. IGARSS 2002 Proceedings Publication:

"A Feasibility Study for a Wide-Swath, Airborne, Hurricane Imaging Microwave Radiometer for Operational Hurricane Measurements," by W. Linwood Jones and Josko Zec (Central Florida Remote Sensing Laboratory, University of Central Florida; Orlando, FL 32816-2450, USA), James W. Johnson (NASA Langley Research Center; Hampton, VA), Christopher S. Ruf (University of Michigan; Ann Arbor, MI), and Marion C. Bailey (Research Triangle Institute; Hampton, VA).

(*see following four pages*)

A Feasibility Study for a Wide-Swath, Airborne, Hurricane Imaging Microwave Radiometer for Operational Hurricane Measurements

W. Linwood Jones, Jun-Dung Park and Josko Zec
University of Central Florida; Orlando, FL
Christopher S. Ruf
University of Michigan; Ann Arbor, MI
Marion C. Bailey
Research Triangle Institute; Hampton, VA
James W. Johnson
NASA Langley Research Center; Hampton, VA

ABSTRACT

This paper presents a conceptual design of an airborne Hurricane Imaging (microwave) Radiometer (HIRad) instrument for use in operational hurricane surveillance. The basis of the HIRad design is the Stepped Frequency Microwave Radiometer (SFMR) that has successfully measured surface wind speed and rain rate in hurricanes from the NOAA Hurricane Research Division's P-3 aircraft. Unlike the SFMR that views only at nadir, the HIRad provides wide-swath measurements between ± 45 degrees in incidence angle with a spot-beam spatial resolution of approximately 1-3 km. The system operates at four equally spaced frequency channels that cover a range between 4 GHz and 7 GHz.

I. INTRODUCTION

Contemporary hurricane numerical models such as MM-5 (Penn State/NCAR Mesoscale Model) have the ability to predict precipitation as well as to forecast storm evolution (intensity, size and track). To aid forecasting, the most important contribution that could be made from remote sensing platforms would be daily mapping of the surface wind field from the center of the storm to a distance just outside the ring of maximum winds located in or near the eyewall cloud. In the Atlantic basin such measurements are operationally available at limited times from sensors mounted on research aircraft, but none of the world's other hurricane basins have aircraft reconnaissance capabilities. Even in the Atlantic hurricanes are out of range of the aircraft for most of their lifetimes. Timely measurements of the surface wind fields in tropical cyclones, with wide swath (10's of km) and high resolution (1 km), would dramatically improve model initialization and resulting forecasts.

II HURRICANE IMAGING RADIOMETER

A. Instrument Heritage

Retrievals of hurricane ocean surface wind speed and rain rate have been performed operationally by the Stepped Frequency Microwave Radiometer (SFMR) from aircraft by NOAA Hurricane Research Division (HRD) for more than a decade. SFMR was originally developed by the NASA Langley Research Center in the 1970s [Jones *et al.*, 1981] and it has continued to be an integral part of NOAA operations since. Wind speed and rain rate are retrieved simultaneously from measurements of microwave brightness temperature (T_B) made by the nadir-viewing SFMR on board a NOAA P-3 flying at ~25,000 ft (7.6 km). Winds in excess of 180 mph (150 m/s) and rain rates of greater than 100 mm/h have been successfully estimated by the SFMR and validated against weather radars, dropsondes released from aircraft, and extrapolations of flight-level winds. Even at these extreme levels, the T_B responses to both wind speed and rain rate have not reached saturation.

The SFMR scans between 5 and 8 GHz with a variable number of channels. Retrievals have been demonstrated with as few as two and as many as eight channels. A minimum of two T_B channels is required to uniquely separate the contrasting spectral signatures of surface emission and rain. Additional channels serve to over-constrain the system of equations that relate the T_B measurements to the state parameters of wind speed and rain rate. This effectively reduces the sensitivity of the retrieval algorithm to instrument noise and common-mode calibration biases. The current operational NOAA sensor uses eight channels.

B. HIRad Instrument Description

The Hurricane Imaging (microwave) Radiometer (HIRad) is a candidate airborne sensor for future operational surface wind speed and rain rate measurements in hurricanes and typhoons. This sensor is an interferometric microwave radiometer that uses a one-dimensional thinned synthetic aperture array antenna to synthesize multiple simultaneous beams in a push-broom configuration. When used on an operational hurricane surveillance aircraft such the NOAA HRD's Gulfstream-IV (Fig. 1), the hurricane may be imaged with high resolution as shown in Fig. 2 & 3.

Unlike the SFMR, that views only at nadir, the HIRad provides wide-swath measurements with simultaneous multiple "pushbroom" fan-beams between ± 45° in incidence angle. When flying at an altitude of 35,000 ft

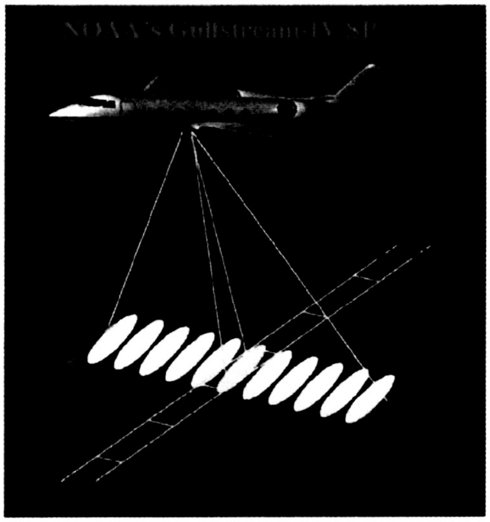

Fig. 1 HIRad measurements from NOAA's hurricane surveillance aircraft.

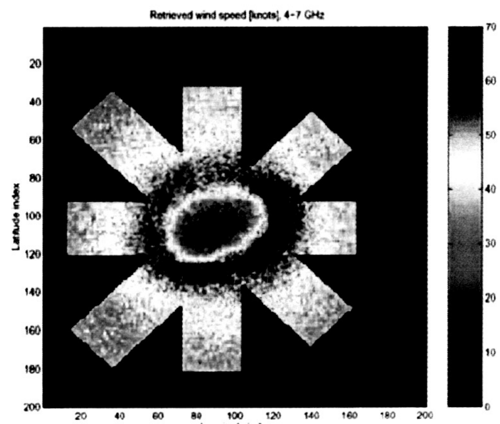

Fig. 2 Simulated HIRad measurements of surface winds from Hurricane Floyd (1999). Ordinate is latitude index (0.125° steps) and the abscissa is longitude index (0.125°). Color scale is 0-70 knts (36 m/s).

(11 km), HIRad provides a measurement swath of 22 km and a spatial resolution of 1-3 km depending upon the operating frequency and cross-track position in the swath. This geometry provides excellent opportunity to image the high wind gradients and spiral rain bands surrounding the hurricane eye while flying the typical "butterfly" transects. The image produced in Fig. 2 and 3 results from four transects of the eye. The advantage of HIRad over a profiling sensor such as SFMR is obvious. The equivalent SFMR coverage would be a single strip (one pixel wide) centered along each the aircraft track.

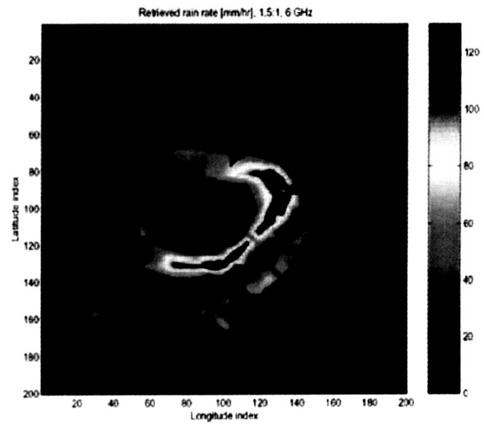

Fig. 3 Simulated HIRad measurements of rain rate from Hurricane Floyd (1999). Color scale is 0-130 mm/hr.

C. Synthetic Thinned Array Radiometer (STAR) System

The STAR instrument design presented here has a frequency plan similar to SFMR but provides a cross track swath at each frequency of 65 independent pixels covering $\pm 45^{\circ}$ about nadir. The pixels are generated using interferometric aperture synthesis [Ruf *et al.*, 1988]. The thinned aperture antenna array consists of 10 active fan beam antennas, each of which is a linear broadside phased array of 36 multi-resonant dipoles (see antenna design section). The linear arrays are oriented in the direction of flight of the aircraft so that their fan beam patterns define the cross track instantaneous field of view of the imager. Full two-dimensional images are then formed by push broom aircraft motion.

The flat panel antenna array (1.1x1.1 m aperture x 25 cm thick) consists of a rectangular grid of 38x38 multi-resonant dipoles with ten receiver front-ends. The small element size (0.4 $\lambda_{free\ space}$ at 4 GHz and 0.7 $\lambda_{free\ space}$ at 7 GHz) allows the design of the array without introduction of grating lobes into the scanning field of view. A multi-slot antenna array element (Fig. 4) is being developed for the 4-7 GHz frequency range. Four resonant frequencies (4, 5, 6 & 7 GHz) were selected for the design. The multi-resonant element is realized by multiple narrow slots in the wall of a specially configured thin cavity. Excitation of the slots is via a stripline inside the cavity and passing directly underneath the slots. Because of the very close proximity of all the slots, there is significant slot-to-slot field interaction. Therefore, the fundamental design was developed and optimized through electromagnetic computational simulations, which model the entire configuration as a single device. Test results on the initial laboratory constructed element demonstrates the four resonant frequencies as predicted. More attention to details in fabrication will be addressed in the next test article in order to improve the impedance match at all frequencies.

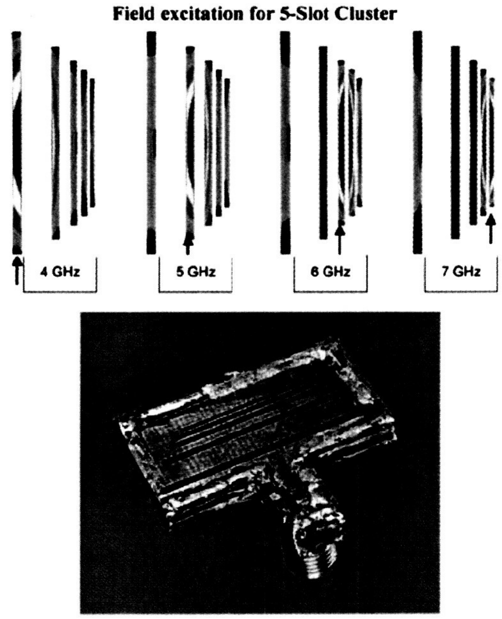

Fig. 4 Antenna element for HIRad array. Top panel illustrates the field excitation and the bottom panel shows a brass-board test article.

The outermost ring of dipoles are passively terminated to ensure consistent mutual coupling between active elements, leaving a 36x36 central grid. The 26 rows of dipoles that do not comprise the 10 active fan beams are also passively terminated. Which 10 of the 36 possible rows are active is determined using an interferometric sampling algorithm [Ruf, 1993].

Each active fan beam antenna is connected to a frequency agile correlating radiometer receiver. The input stage of each receiver features a reference load and injected noise diode for absolute system calibration followed by a wideband low noise amplifier covering the 4-7 GHz input frequency range. The frequency selection is achieved by single sideband downconversion to a fixed narrowband (20 MHz) intermediate frequency (IF) range using a variable local oscillator, in a manner adapted from the SFMR design. The IF signal is digitized (prior to detection) with a coarse 2-bit digitizer and then digitally quadrature demodulated to baseband and complex cross-correlated between receivers using technology and signal processing algorithms developed under a NASA Global Precipitation Measurement Mission technology development incubator [Ruf *et al.*, 2000].

D. *HIRad Simulated Performance Results*

HIRad hurricane measurements are simulated using a statistical Monte Carlo technique. The wide-swath coverage provided from typical aircraft altitudes is capable of mapping the entire hurricane eye wall during a few flight tracks across the storm. These simulated retrievals show good accuracy for surface wind speed and rain rate under realistic hurricane conditions. An example of the spatial distribution of retrieval errors is presented in Fig. 5. The top panel is the modeled wind field with the error in the retrieved wind speed directly below. The maximum errors ~ 5 m/s occur at light winds inside of the eye, and at stronger winds where the system is optimized, the error is less. Also note that the wind speed errors are not correlated with the location of strong rain (panel 3rd from top). Directly below the model rain intensity is the rain rate retrieval error. Again the largest errors are for light rains inside of the eye, and for stronger rains, where the system is optimized, the errors are less. Also note that rain rate errors are independent of wind speed. Scatter diagrams of the wind speed and rain rate retrieval errors are presented in Fig. 6 for the entire hurricane. As discussed above, the errors reduce as the wind speed and rain rate increase. At light winds and rain there is a sensitivity issue because of selecting the low frequency microwave channels (4 GHz - 7 GHz). However, at the strong wind speeds and rain intensity associated with tropical cyclones there is an exponential increase in T_b with these increasing parameters, and the retrievals improve.

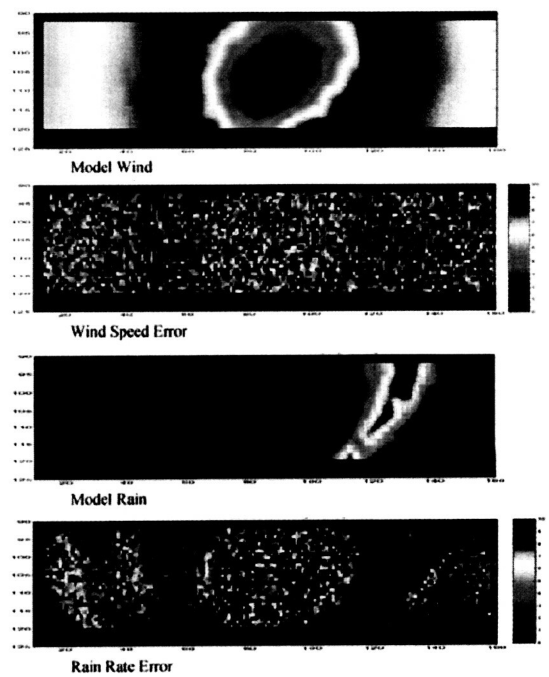

Fig. 5 HIRAD simulated east-West flight leg. Top panel is the modeled wind speed; next is the retrieved wind speed error - color bar is 0-10 knts (5.2 m/s), next is the modeled rain intensity and the bottom panel is the corresponding rain rate retrieval error - color bar is 0-10 mm/hr.

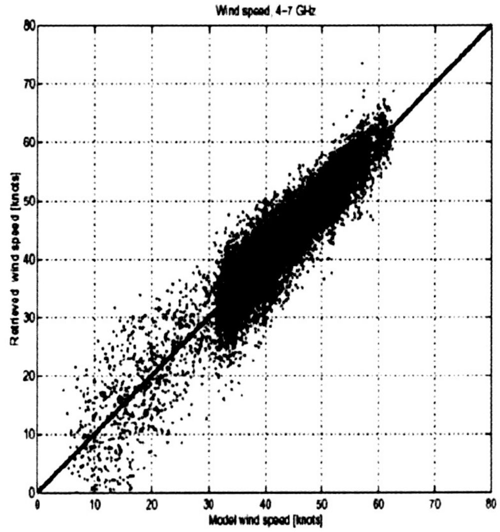

(a) - HIRad wind speed error - entire hurricane image

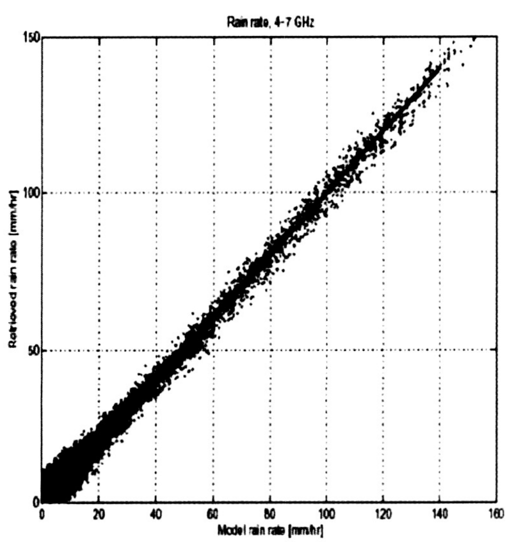

Fig. 6 HIRAD simulated hurricane retrieval error. Top panel is the wind speed error and the bottom panel is the corresponding rain rate error

III Conclusions

This design study has demonstrated the feasibility of developing a new Hurricane Imagine Radiometer using currently available technologies for Synthetic Thinned Array Radiometers. There is significant potential for this candidate airborne sensor for future operational surface wind speed and rain rate measurements in hurricanes and typhoons.

Acknowledgment

This work was performed under a Research triangle institute contract with NASA Langley Research Center.

References

Jones, W.L., P.G. Black, V.E. Delnore, and C.T. Swift (1981). "Airborne Microwave Remote Sensing Measurements of Hurricane Allen," Science, 214, 274-280.

Ruf, C.S., C.T. Swift, A.B. Tanner and D.M. Le Vine, "Interferometric synthetic aperture microwave radiometry for the remote sensing of the earth," IEEE Trans. Geosci. Remote Sens., 26(5), 597-611, 1988.

Ruf, C.S., "Numerical annealing of low redundancy linear arrays," IEEE Trans. Antennas and Propag., 41(1), 85-90, 1993.

Ruf, C.S., C.M. Principe and S.P. Neeck, "Enabling Technologies to Map Precipitation with Near-Global Coverage and Hour-Scale Revisit Times," Proceedings of the 2000 International Geoscience and Remote Sensing Symposium, Honolulu, HI, IEEE Cat. #99CH37120, Vol. VII, 2988-2990, 2000.

3.1. Overview

This document summarizes the design of a MMIC Radiometer Front End as of August 22, 2002. Specifically, preliminary design information and Agilent ADS 2002 simulation results for the LNA, IF Mixer, and IF Amp are included.

3.2. System Design

The MMIC Radiometer Front End was targeted for Triquint's TQTRx process. This process was selected because of its frequency range and the free availability of the model library.

3.2.1. System Block Diagram

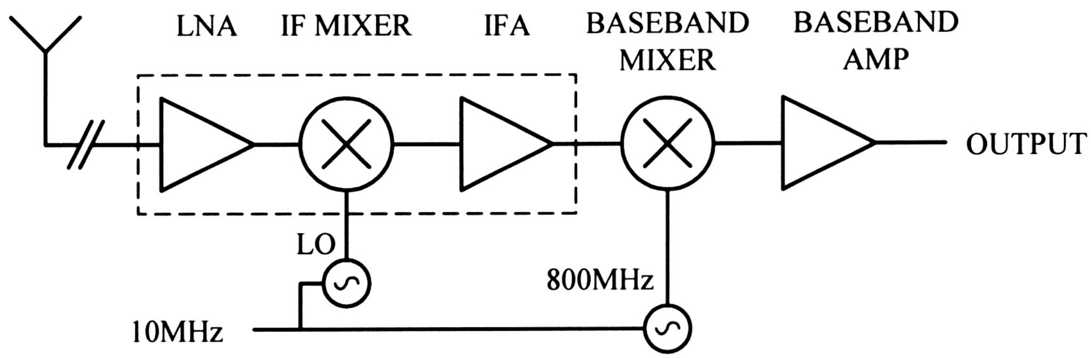

3.2.2. System Specification

RF Bandwidth:	4-9 GHz (-3 dB)
Gain:	83.5 dB
Gain Flatness:	+/- 1 dB
Baseband:	100-300 MHz (-3 dB)
Noise Figure:	< 3 dB
DC Power:	580 mW
Image Rejection:	< -10 dB (USB/LSB)
Input Return Loss:	< -10 dB

3.2.3. System Simulation Results

Lower Side Band Gain

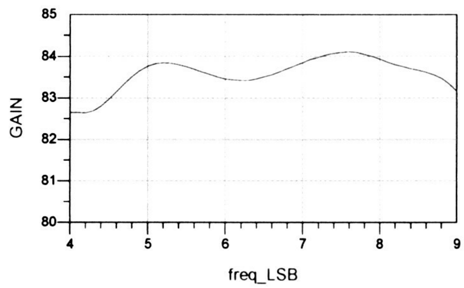

Image Rejection Ratio (USB/LSB)

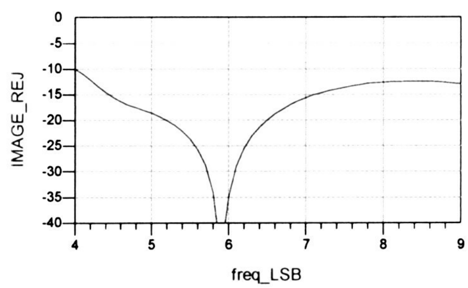

DC Power

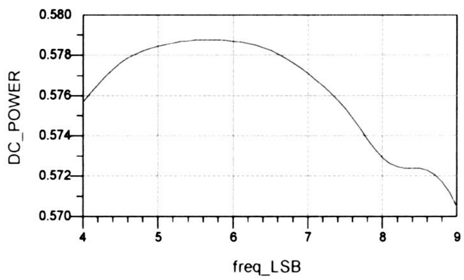

Input Return Loss

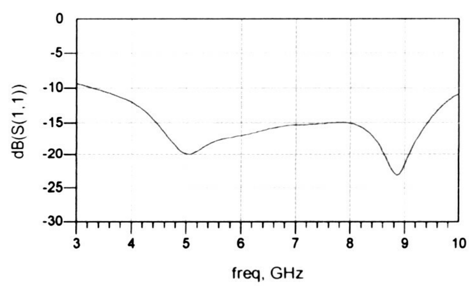

Output Return Loss

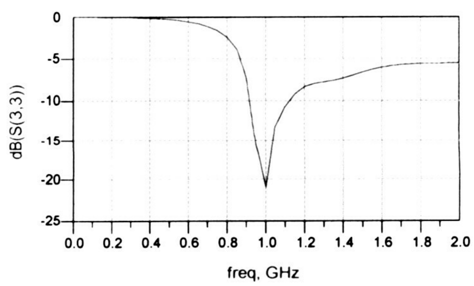

3.3 LNA Design

A three-transistor common-source cascaded design was initially attempted. While capable of enough gain and low noise figure it was found impossible to meet bandwidth requirements. A distributed topology was then attempted. The distributed topology allows greater than octave bandwidth as well as high gain by trading off chip size and power consumption.

The distributed topology is characterized by multiple FETs connected by transmission lines of equal phase delay from successive gate to gate and drain to drain [1]. Equal phase delay is accomplished by equal length microstrip between transistors as well as a compensation capacitor equaling the difference between Cgs and Cds. This has the effect of summing the gain from each successive transistor in-phase. Thus, by keeping the gain of each transistor low (~2 dB) a very large gain-bandwidth product is produced. Further, the input and output matches are very good as both the drain and gate transmission lines were designed to be 50 ohms. This design performs similarly with 1nH spiral inductors in place of the 900um long microstrip sections, as well as 500pH spiral inductors in place of the 425um long sections.

To meet the total gain requirement three sections of the circuit shown below are cascaded. This is illustrated in Appendix A along with biasing information.

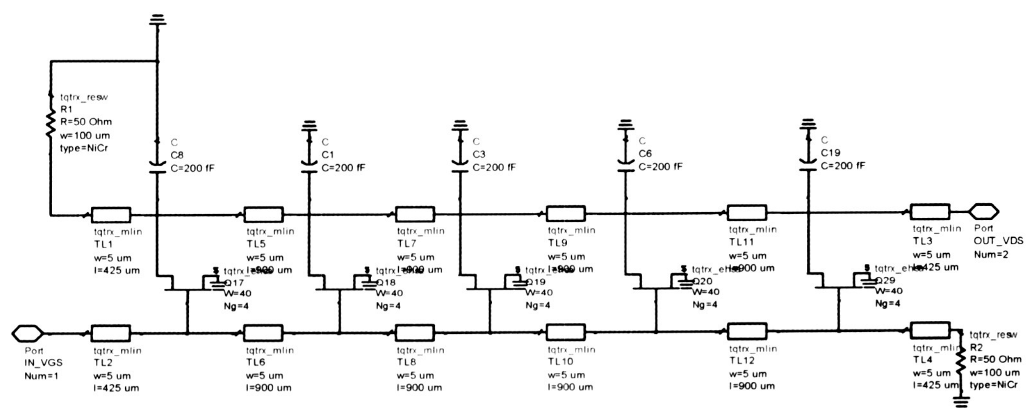

3.3.1. Specification

Gain:	33 dB, from 4-9 Ghz (-3dB)
Gain Flatness:	+/- 1.5dB (max)
Noise Figure:	< 3 dB, from 4-9 Ghz
DC Power:	340 mW
Input Return Loss:	< -10 dB, from 4-9 Ghz
Output Return Loss:	< -10 dB, from 4-9 Ghz

3.3.2. LNA Simulation Results

Gain, Noise Figure, Input Return Loss, Output Return Loss

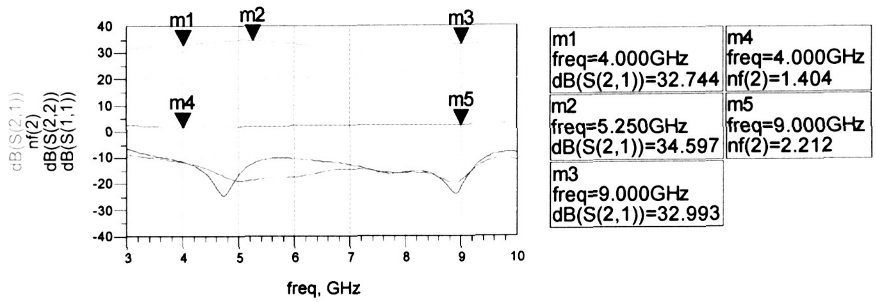

DC Power

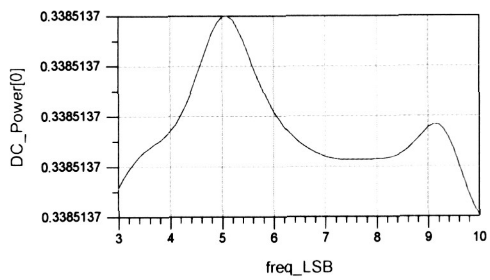

3.4 IF Mixer Design

Due to the system requirements it is necessary that the IF Mixer provide single side band down conversion. One way of attempting this is by providing a low pass filter to discriminate against the upper side band and passing the lower side band. However, because of the high bandwidth a tunable filter capable of greater than octave bandwidth would be necessary. This was deemed excessively complex. Instead, a design providing single side band down conversion through selective phase cancellation of the undesired sideband was performed [2].

At the input to the IF Mixer is a -90 degree wideband coupler. This splits the input RF signal into a 0 degree phase signal and -90 degree phase signal. Each of these signals is then fed to identical single-ended mixer stages, which perform dual side band down conversion. The single-ended mixer fed the 0 degree RF signal reproduces the upper sideband at the IF with 0 degree phase and the lower sideband with 180 degree phase. The single-ended mixer fed the -90 degree RF signal reproduces the upper sideband at the IF with -90 degree phase and the lower sideband with 90 degree phase. When these signals are fed to the 90 degree 1 GHz coupler at the output one portion of the upper sideband is coupled through and one portion receives a -90 degree phase shift. When the 0 degree upper sideband is combined with the now -180 degree upper sideband phase cancellation occurs. Conversely, the lower sideband is reproduced at the IF when its two portions are combined in phase. The difference in output power at the IF between the lower sideband and the upper sideband is known as the image rejection ratio. The image rejection ratio is a function of the phase difference imparts on the signals by the couplers and the magnitude of the difference in coupling.

Full schematics are contained in Appendix B.

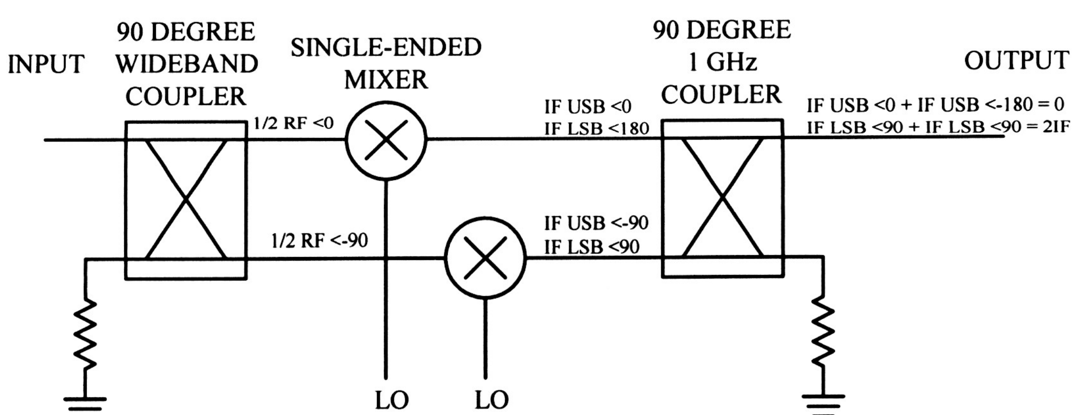

3.4.1. Specification

Conversion Loss:	> -10 dB
Image Rejection Ratio:	< -10 dB
RF Return Loss:	< -10 dB
IF:	900-1100 MHz (-3 dB)

3.4.2. Simulation Results

Conversion Loss and Image Rejection
LO swept 1 GHz above LSB
USB swept 2 GHz above LSB

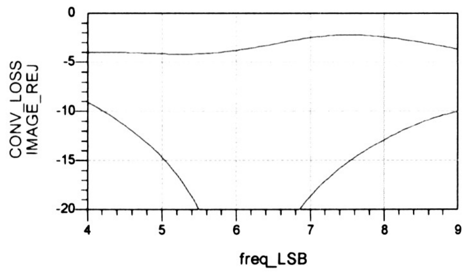

Conversion Loss and Image Rejection
LO fixed at 7 GHz

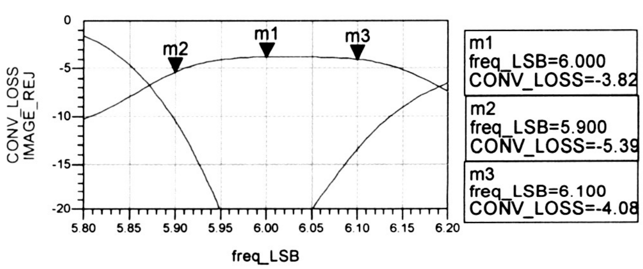

RF Port Return Loss

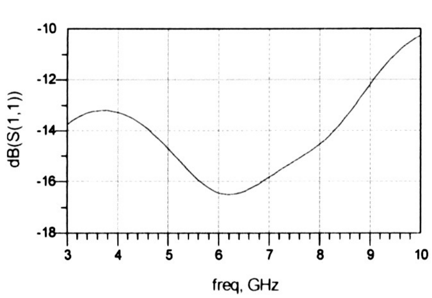

IF Port Return Loss

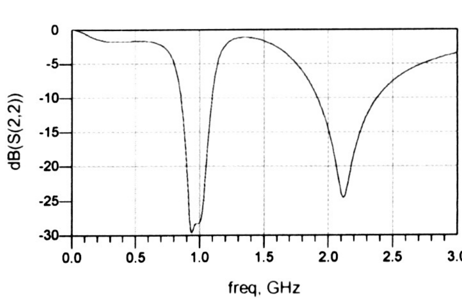

3.5. IF Amp

The IF Amp is a classic common-source cascaded design. One small difficulty encountered in the design is the 20% bandwidth at a frequency low for the process. Additionally, it would be desirable to reduce the gain above the IF as much as possible to aboive risking instability by amplifying undesired harmonics from the mixer, primarily the LO. This is not expected to be a large problem, however, as the lowest frequency of the LO is 5 GHz, well above the IF, and may simply be filtered out.

A full schematic is in Appendix C.

3.5.1. Specification

Bandwidth:	900-1100 MHz (-3 dB)
Gain:	> 50 dB
Gain Compression:	> 0 dBm (-1 dB)
Noise Figure:	< 10 dB
DC Power:	< 300 mW

3.5.3. Simulation Results

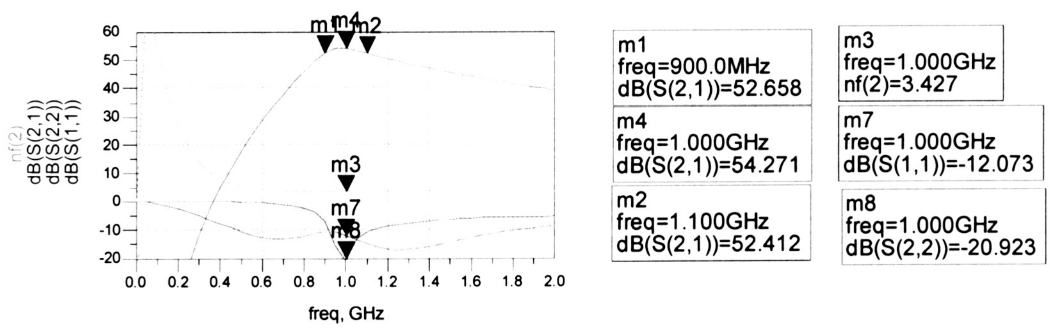

More complete simulation results are contained in Appendix C.

3.6.1. Appendix A: LNA Detail

LNA Biasing and Stage Interconnection

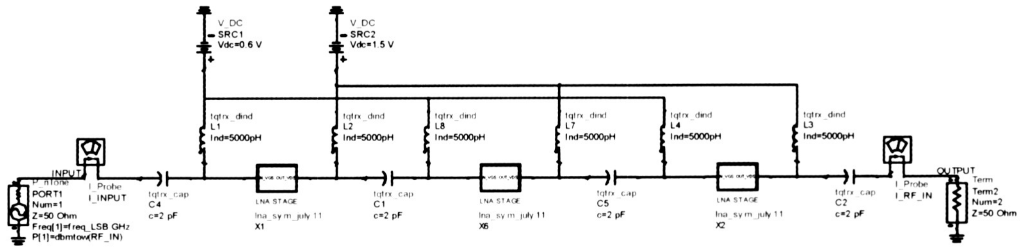

Input Stability

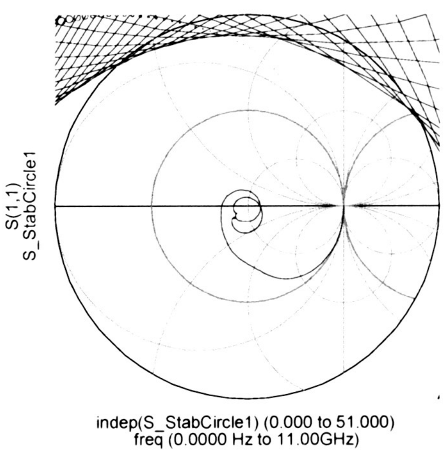

Output Stability

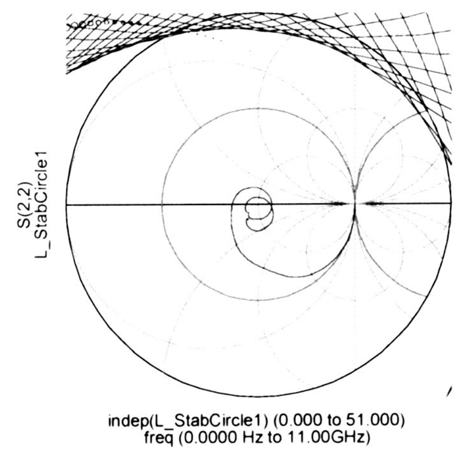

P-1dB, OIP2, OIP3

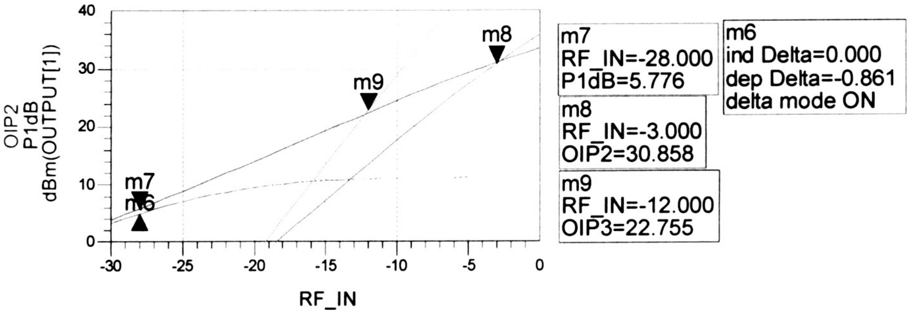

3.6.2. Appendix B: Mixer Detail

Full Schematic

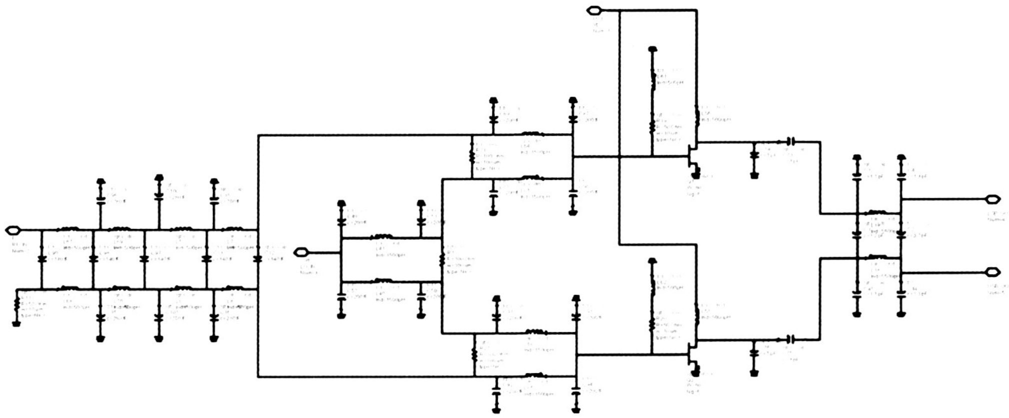

90 Degree Wideband Coupler

Schematic

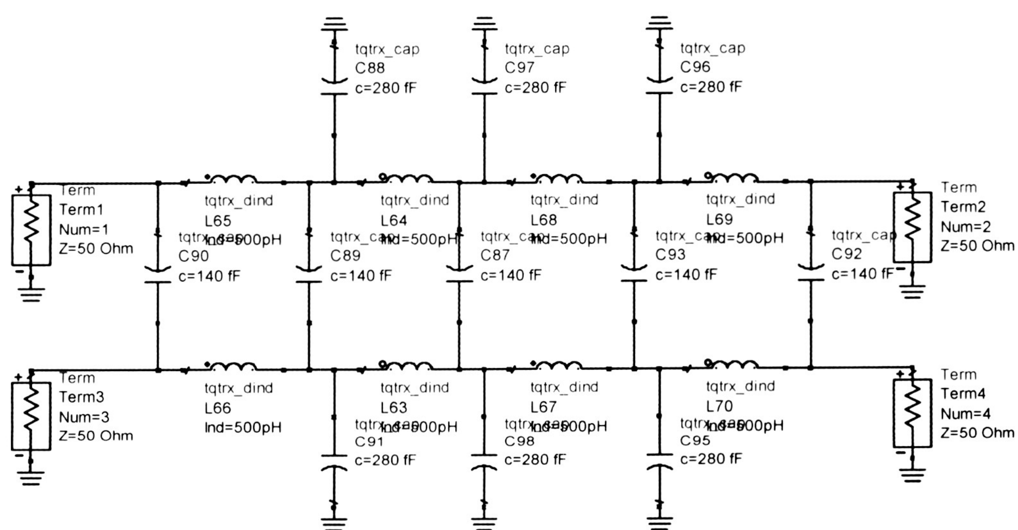

Simulation Results of 90 Degree Wideband Coupler

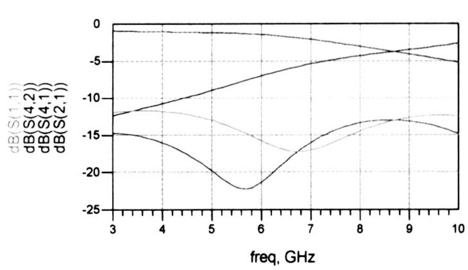

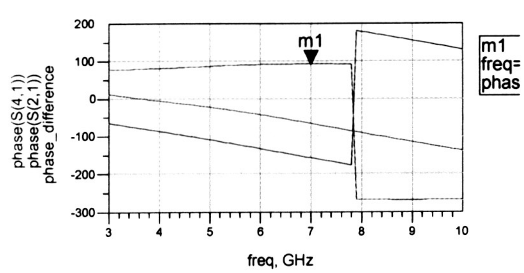

Single Ended Mixer

Schematic

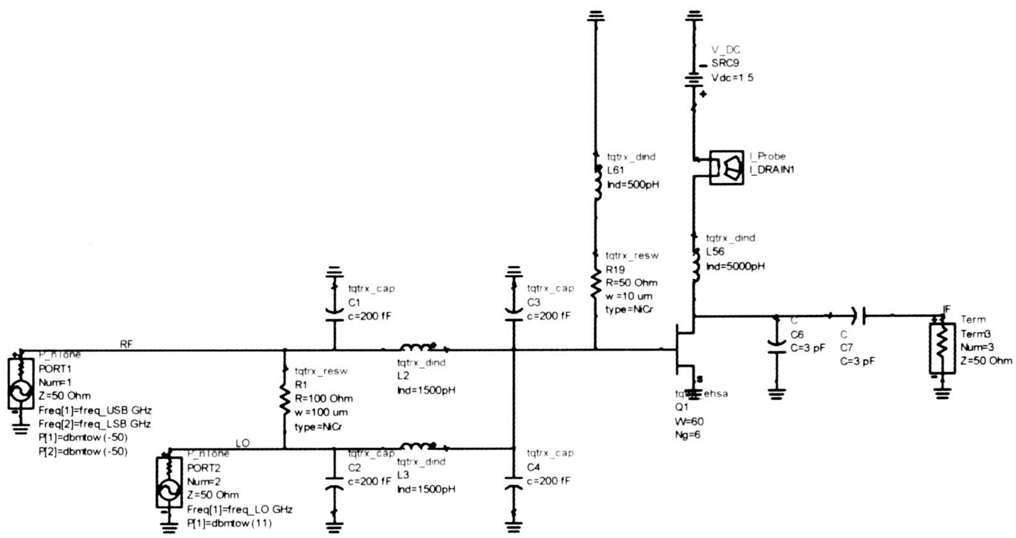

Simulation Results

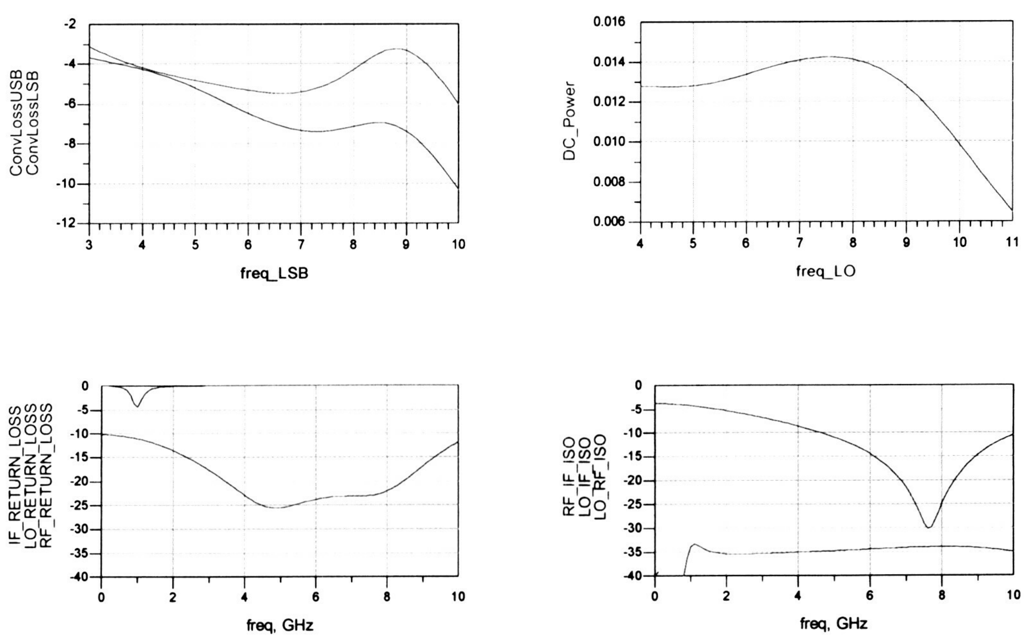

90 Degree 1 GHz Coupler

Schematic

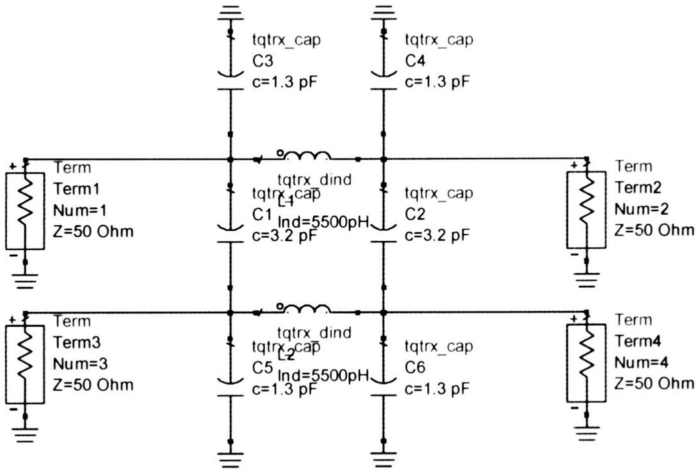

Simulation Results

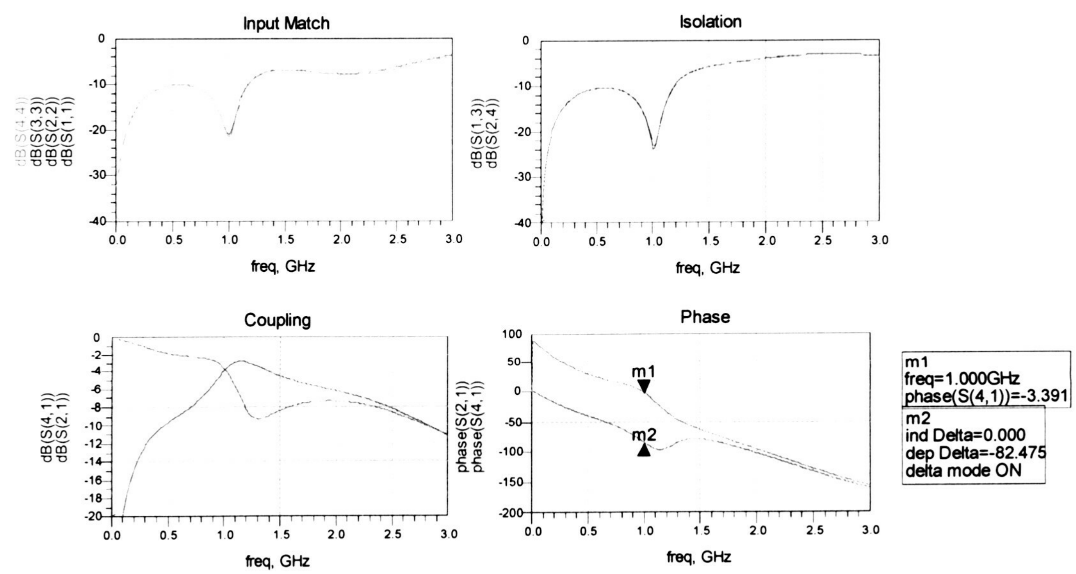

3.6.3. Appendix C: IFA Detail

Input Stability

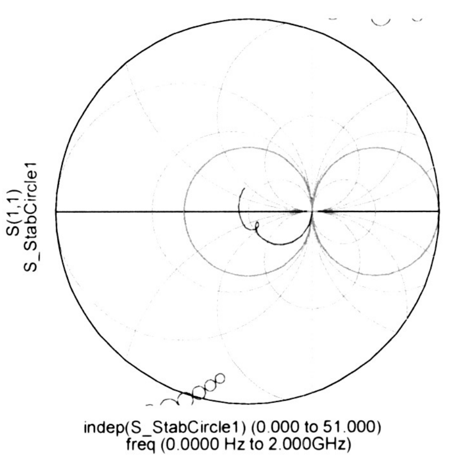

Output Stability

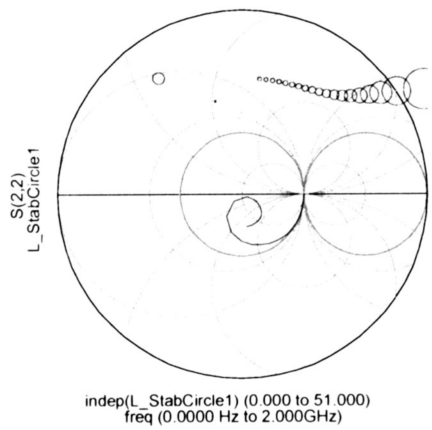

P-1dB, OIP2, OIP3

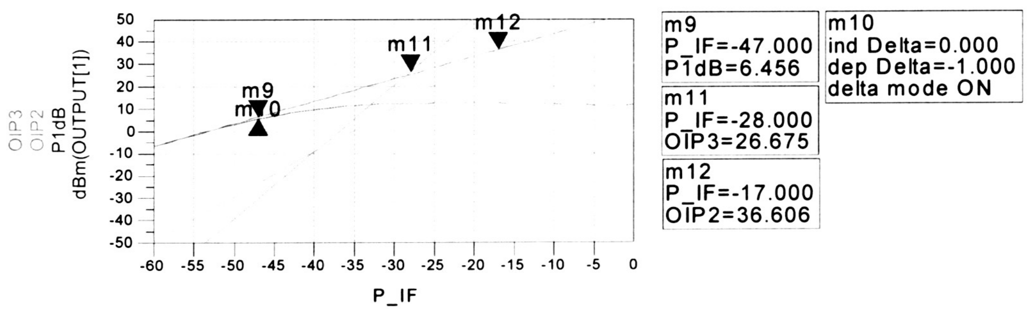

DC Power

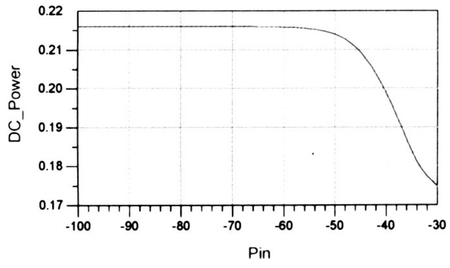

3.7. References

[1] A. A. Sweet, *MIC and MMIC Amplifier and Oscillator Circuit Design*, pp. 120-128, Norwood, MA: Artech House, 1990.

[2] S. A. Maas, *Microwave Mixers*, pp. 280-283, Norwood, MA: Artech House, 1993.

4. Publications and conference/workshop presentations generated by this project

Jones, W.L., J.-D. Park, J. Zec, C.S. Ruf, M.C. Bailey and J.W. Johnson, "A Feasibility Study for a Wide-Swath, Airborne, Hurricane Imaging Microwave Radiometer for Operational Hurricane Measurements," Proc. of the 2002 IEEE International Geoscience and Remote Sensing Symposium, Toronto, CA, 24-28 June 2002, IEEE Cat. #02CH37380, 2002.

Jones, W.L., J. Zec, J.W. Johnson, C. S. Ruf and M.C. Bailey, "A Feasibility Study for a Wide-Swath, High Resolution, Airborne Microwave Radiometer for Operational Hurricane Measurements," Proc. of the 56th Interdepartmental Hurricane Conference, 11-15 March 2002, New Orleans, LA, 2002.